Article

SHM Structural Health Monitoring

Structural Health Monitoring
10(5) 539–553

DOI: 10.1177/1475921710388972
shm.sagepub.com
SAGE

# Q-statistic and $T^2$-statistic PCA-based measures for damage assessment in structures

**LE Mujica[1], J Rodellar[1], A Fernández[2] and A Güemes[2]**

**Abstract**

This article explores the use of principal component analysis (PCA) and $T^2$ and $Q$-statistic measures to detect and distinguish damages in structures. For this study, two structures are used for experimental assessment: a steel sheet and a turbine blade of an aircraft. The analysis has been performed in two ways: (i) by exciting the structure with low-frequency vibrations using a shaker and using several piezoelectric (PZT) sensors attached on the surface, and (ii) by exciting at high-frequency vibrations using a single PZT as actuator and several PZTs as sensors. A known vibration signal is applied and the dynamical responses are analyzed. A PCA model is built using data from the undamaged structure as a reference base line. The defects in the turbine blade are simulated by attaching a mass on the surface at different positions. Instead, a progressive crack is produced to the steel sheet. Data from sets of experiments for undamaged and damaged scenarios are projected into the PCA model. The first two projections, and the $Q$-statistic and $T^2$-statistic indices are analyzed. $Q$-statistic indicates how well each sample conforms to the PCA model. It is a measure of the difference or residual between a sample and its projection into the principal components retained in the model. $T^2$-statistic index is a measure of the variation of each sample within the PCA model. Results of each scenario are presented and discussed demonstrating the feasibility and potential of using this formulation in structural health monitoring.

**Keywords**

damage detection, principal component analysis, aircraft structures

## Introduction

Nowadays, the aerospace and aircraft industry has a main priority in improving the reliability of their structures through the development of novel systems for monitoring and damage detections. In the last years, significant efforts are being concentrated in the design of smart structures with the integration of materials, sensors, actuators, and algorithms able to monitor the structural state health in real time and detect any defect at an early stage.[1] The basic paradigm is to approach the damage identification via the detection of changes in the propagation of elastic waves through the structure by analyzing time responses in comparison with pattern responses for undamaged structures.[2]

There are several potentially useful techniques, and their applicability to a particular situation depends on the size of critical damage admissible in the structure. All of these techniques follow the same general procedure: the structure is excited using actuators and the dynamical response is sensed at different locations throughout the structure. Any damage will change this vibrational response, as well as the transient by a wave that is spreading through the structure. The state of the structure is diagnosed by means of the processing of these data. Correlating the signals to detect, locate and quantify these changes is a very complex problem, but very significant progresses have been recently reported in conferences,[3–5] new scientific journals,[6,7] and books.[8,9]

In general, there are many ways to tackle the problem, Farrar et al. defined the process in terms of a four-step statistical pattern recognition paradigm which

[1]Department of Applied Mathematics III, Universitat Politécnica de Catalunya, Comte d'Urgell 187, 08036 Barcelona, Spain.
[2]Department of Aeronautics, Universidad Politécnica de Madrid, Plaza Cisneros 3. 28040 Madrid, Spain.

**Corresponding author:**
L.E. Mujica, Department of Applied Mathematics III, Universitat Politécnica de Catalunya, Comte d'Urgell 187, 08036 Barcelona, Spain
Email: luis.eduardo.mujica@upc.edu

includes: (i) operational evaluation, (ii) data acquisition, normalization and cleansing, (iii) feature selection and information condensation, and (iv) statistical model development for feature discrimination.[10]

According to theories summarized by McCullagh,[11] in the strict sense, a statistical model is a set of mathematical expressions that describe the behavior of an object to study in terms of random variables and their associated probability distributions on the sample space. In other words, the probability theory is applied to a set of data in order to get an algorithm. This is opposed to using training data to select among different algorithms or using heuristics/common-sense to design an algorithm. In the literature, many methods can be found to determine a statistical model, for instance: linear, basis function and Gaussian regressions; feed-forward neural networks; linear classifiers, support vector machine, Markov models, principal component analysis (PCA), etc.

In structural health monitoring (SHM), PCA[12] has been extensively applied to measured vibration signals for dimensionality studies,[13–15] to remove the influence of the environmental effects from the vibration characteristics,[16,17] for extracting structural damage features,[18–20] to discriminate features from damaged and undamaged structures[21–25] and for clustering a classification of acoustic emission transient,[26] among others.

In the above references, concerning PCA analysis, just the principal components or the projections to these principal components are studied. However, there exist other PCA-related tools that also give information about what is going within the model. The goal of this article is to explore the potential of two statistical distances to detect and distinguish structural damages. The study is experimentally based considering two test cases. The article first presents a background on the basic concepts on PCA and the damage detection indices in sections 'Principal component analysis' and 'Damage detection indices'. The methodology for a systematic implementation of the approach for damage diagnosis is outlined in section 'Methodology for structural health monitoring'. The experimental settings are described in section 'Experimental set-up' and the results are discussed in section 'Analysis of the results'. Finally, some concluding remarks are summarized in section 'Concluding remarks'.

## Principal component analysis

### Introduction

In many scientific fields, including SHM, it is common to deal with a large variety of complex systems in which the number of variables to measure can be unwieldy and even at some times deceptive, because the implicit relationships can often be quite simple. PCA may provide arguments for how to reduce a complex data set to a lower dimension and reveal some hidden and simplified structure/patterns that often underlie it. The goal of PCA is to discern which dynamics are more important in the system, which are redundant and which are just noise. This goal is essentially achieved by determining a new space (coordinates) to re-express the original data filtering that noise and redundancies based on the variance–covariance structure of the original data. PCA can be also considered as a simple, nonparametric method for data compression and information extraction, which finds combinations of variables or factors that describe major trends in a confusing data set.[1]

### Data collection

Let us address the analysis of a physical process by measuring several variables (sensors) at a number of time instants (or experimental trials), considering that each measurement is an individual sample in the data set (just one value, e.g., load, voltage, pressure, etc.). The collected data are arranged in a matrix as follows:

$$\mathbf{X} = \begin{pmatrix} x_{11} & x_{12} & \dots & x_{1j} & \dots & x_{1m} \\ \dots & \dots & \dots & \dots & \dots & \dots \\ x_{i1} & x_{i2} & \dots & x_{ij} & \dots & x_{im} \\ \dots & \dots & \dots & \dots & \dots & \dots \\ x_{n1} & x_{n2} & \dots & x_{nj} & \dots & x_{nm} \end{pmatrix} = \left(\boldsymbol{v}_1 \middle| \boldsymbol{v}_2 \middle| \cdots \middle| \boldsymbol{v}_j \middle| \cdots \middle| \boldsymbol{v}_m\right) \quad (1)$$

This $n \times m$ matrix contains information from $m$ sensors and $n$ experimental trials. Each row vector ($\boldsymbol{x}_i$) represents measurements from all the sensors at a specific time instant or experiment trial. In the same way, each column vector ($\boldsymbol{v}_j$) represents measurements from one sensor (one variable) in the whole set of experiment trials.

### Scaling

Since different physical variables and sensors have different magnitudes and scales, the original data set has to be treated before applying any analysis. Several methods are found in the literature for scaling experimental data, the so-called 'autoscaling' being the most popular. It is a processing technique in which each variable is re-scaled to have zero mean and unity variance. This is performed by modifying each sensor vector $\boldsymbol{v}_j$ as follows:

$$\mu_{v_j} = \frac{1}{n}\sum_{i=1}^{n} x_{ij}, \quad (2)$$

$$\sigma_{v_j}^2 = \frac{1}{n-1}\sum_{i=1}^{n}\left(x_{ij}-\mu_{v_j}\right)^2, \tag{3}$$

$$\bar{x}_{ij} = \frac{x_{ij}-\mu_{v_j}}{\sigma_{v_j}}, \tag{4}$$

where $\mu_{vj}$ and $\sigma_{v_j}^2$ are the mean and the variance, respectively, of sensor $j$ measurements ($\boldsymbol{v}_j$), and $\bar{x}_{ij}$ is the re-scaled sample. In the remaining of the article the scaled data are considered without bar notation for simplicity.

### Covariance matrix and PCA objective

Given a data matrix $\mathbf{X}$ in (1), which has been previously scaled, the covariance matrix is defined as follows:

$$\mathbf{C}_\mathrm{X} \equiv \frac{1}{n-1}\mathbf{X}^\mathrm{T}\mathbf{X} = \frac{1}{n-1}\begin{pmatrix} \boldsymbol{v}_1^T\boldsymbol{v}_1 & \boldsymbol{v}_1^T\boldsymbol{v}_2 & \dots & \boldsymbol{v}_1^T\boldsymbol{v}_j & \dots & \boldsymbol{v}_1^T\boldsymbol{v}_m \\ \dots & \dots & \dots & \dots & \dots & \dots \\ \boldsymbol{v}_j^T\boldsymbol{v}_1 & \boldsymbol{v}_j^T\boldsymbol{v}_2 & \dots & \boldsymbol{v}_j^T\boldsymbol{v}_j & \dots & \boldsymbol{v}_j^T\boldsymbol{v}_m \\ \dots & \dots & \dots & \dots & \dots & \dots \\ \boldsymbol{v}_m^T\boldsymbol{v}_1 & \boldsymbol{v}_m^T\boldsymbol{v}_2 & \dots & \boldsymbol{v}_m^T\boldsymbol{v}_j & \dots & \boldsymbol{v}_m^T\boldsymbol{v}_m \end{pmatrix} \tag{5}$$

It is a square symmetric $m \times m$ matrix that measures the degree of linear relationship within the data set between all possible pairs of variables (sensors). The diagonal terms are the variances of the corresponding variables:

$$\sigma_{v_j}^2 = \frac{1}{n-1}\boldsymbol{v}_j^T\boldsymbol{v}_j = \frac{1}{n-1}\sum_{i=1}^{n}x_{ij}^2 \tag{6}$$

When dealing with measured data, it is important to have low noise levels if valuable information is wanted to be extracted. Noise cannot be directly measured, but a common estimation, relative to the measurement, is the signal-to-noise ratio ($\mathrm{SNR} = \sigma^2{}_\mathrm{s}/\sigma^2{}_n$), which compares the variances of the signal and the noise. The larger the SNR is, the more accurate the data are. Therefore, measurement vectors with larger variances within the data set contain more interesting dynamics.

The off-diagonal terms are the covariance between pairs of variables:

$$\sigma_{v_j,v_k}^2 = \frac{1}{n-1}\boldsymbol{v}_j^T\boldsymbol{v}_k = \frac{1}{n-1}\sum_{i=1}^{n}x_{ij}x_{ik} \tag{7}$$

Large covariance values correspond to high redundancy and small values to low redundancy.

Looking at the structure of the data matrix $\mathbf{X}$, we may see all the row vectors $\boldsymbol{x}_i$ as lying in an $m$-dimensional space spanned with the natural orthonormal basis of vectors $(1,0,\dots,0)$, $(0,1,0,\dots,0)$ to $(0,0,\dots,1)$. In this algebraic context, it is worth to consider transforming the vectors $\boldsymbol{x}_i$ and the data matrix $\mathbf{X}$ to be expressed in a different orthonormal basis, in which the modified data better exhibits some desired features. According to the above noise/redundancy issues, the goal of PCA is to re-express the original data in a new basis where the data are arranged along directions of maximal variance and minimal redundancy.

### Transforming the data matrix

Consider a $m \times n$ linear transformation matrix $\mathbf{P}$, which is used to transform the original data matrix $\mathbf{X}$ into the form:

$$\mathbf{T} = \mathbf{XP} \tag{8}$$

To achieve the minimal redundancy goal, we seek for a transformation matrix $\mathbf{P}$ such that the covariance of the new data matrix $\mathbf{T}$ is diagonal, that is:

$$\mathbf{C}_\mathrm{T} = \frac{1}{n-1}\mathbf{T}^\mathrm{T}\mathbf{T} = \text{diagonal} \tag{9}$$

Substituting (8) into (9) the following is written:

$$\mathbf{C}_\mathrm{T} = \frac{1}{n-1}\mathbf{P}^\mathbf{T}\mathbf{X}^\mathbf{T}\mathbf{X}\mathbf{P} = \mathbf{P}^\mathbf{T}\mathbf{C}_\mathbf{X}\mathbf{P} \tag{10}$$

Since $\mathbf{C}_\mathbf{X}$ is symmetric, it has $m$ real eigenvalues $\lambda_j$ and $m$ orthonormal eigenvectors $\boldsymbol{p}_j$, which form a basis in the $m$-dimensional space. Then, the transformation matrix is chosen having the eigenvectors in their columns, that is:

$$\mathbf{P} = \left(\boldsymbol{p}_1|\boldsymbol{p}_2|\dots|\boldsymbol{p}_j|\dots|\boldsymbol{p}_m\right) \tag{11}$$

With this matrix the following property is satisfied:

$$\mathbf{C}_\mathbf{X}\mathbf{P} = \mathbf{P}\Lambda \tag{12}$$

with $\Lambda = \mathrm{diag}(\lambda_1, \lambda_2, \dots, \lambda_m)$. Substituting (12) into (10), the desired condition (9) is satisfied with:

$$\mathbf{C}_\mathbf{T} = \mathbf{P}^\mathbf{T}\mathbf{P}\Lambda = \Lambda \tag{13}$$

Let us write the transformation (8) in more detail:

$$\left(\boldsymbol{t}_1|\{\boldsymbol{t}_2|\ldots|\boldsymbol{t}_j|\ldots|\boldsymbol{t}_m\right) = \begin{pmatrix} x_{11} & x_{12} & \ldots & x_{1j} & \ldots & x_{1m} \\ \ldots & \ldots & \ldots & \ldots & \ldots & \ldots \\ x_{i1} & x_{i2} & \ldots & x_{ij} & \ldots & x_{im} \\ \ldots & \ldots & \ldots & \ldots & \ldots & \ldots \\ x_{n1} & x_{n2} & \ldots & x_{nj} & \ldots & x_{nm} \end{pmatrix} \times \left(\boldsymbol{p}_1|\boldsymbol{p}_2|\ldots|\boldsymbol{p}_j|\ldots|\boldsymbol{p}_m\right) \quad (14)$$

Each column vector in matrix $\mathbf{T}$ can be expressed as:

$$\boldsymbol{t}_j = \mathbf{X}\boldsymbol{p}_j \quad (15)$$

Then, the variances of these vectors can be computed in the form:

$$\sigma_{t_j}^2 = \frac{1}{n-1}\boldsymbol{t}_j^T\boldsymbol{t}_j = \frac{1}{n-1}\left(\mathbf{X}\boldsymbol{p}_j\right)^T\left(\mathbf{X}\boldsymbol{p}_j\right) = \boldsymbol{p}_j^T\mathbf{C}_\mathbf{X}\boldsymbol{p}_j = \lambda_j \quad (16)$$

while the covariances are null:

$$\sigma_{t_j,t_k}^2 = \frac{1}{n-1}\boldsymbol{t}_j^T\boldsymbol{t}_k = \frac{1}{n-1}\left(\mathbf{X}\boldsymbol{p}_j\right)^T\left(\mathbf{X}\boldsymbol{p}_k\right) = \boldsymbol{p}_j^T\mathbf{C}_\mathbf{X}\boldsymbol{p}_k = \lambda_j\boldsymbol{p}_j^T\boldsymbol{P}_k = 0 \quad (17)$$

Consequently, the row vectors of the transformed data matrix $\mathbf{T}$ are uncorrelated and their respective variances are given by the eigenvalues of the covariance matrix $\mathbf{C}_\mathbf{x}$ of the original data. Usually the eigenvectors $\boldsymbol{p}_j$ forming the transformation matrix $\mathbf{P}$ are sorted according to the eigenvalues by descending order and they are called the Principal Components of the data set. The eigenvector with the highest eigenvalue represents the most important pattern in the data with the largest quantity of information.

Geometrically, the $j$th-column vector $\boldsymbol{t}_j$ of the transformed data matrix $\mathbf{T}$ is the projection of the original data over the direction of vector $\boldsymbol{p}_j$ ($j$th principal component). Intuitively speaking, matrix $\mathbf{T}$ gives a new representation of the data set as 'seen' by 'virtual sensors' in a nonphysical space, where the corresponding 'virtual variable vectors' are uncorrelated and have the maximal data variance, thus with best potential to exhibit process features.

## Reducing the dimension

Since eigenvectors are ordered according to the amount of information, it is possible to reduce the dimensionality of the data set $\mathbf{X}$ by choosing only a reduced number $r$ of principal components, those corresponding to the first eigenvalues. Thus, define the following reduced transformation $m \times r$ matrix:

$$\mathbf{P} = \left(\boldsymbol{p}_1|\boldsymbol{p}_2|\ldots|\boldsymbol{p}_r\right) \quad (18)$$

Then the original data can be projected onto the space spanned by this matrix as before:

$$\mathbf{T} = \mathbf{X}\mathbf{P} \quad (19)$$

In the full dimension case, this projection is invertible (since $\mathbf{P}\mathbf{P}^\mathbf{T} = \mathbf{I}$) and the original data can be recovered as $\mathbf{X} = \mathbf{T}\mathbf{P}^\mathbf{T}$. Now, with the given $\mathbf{T}$, it is not possible to fully recover $\mathbf{X}$, but $\mathbf{T}$ can be projected back onto the original $m$-dimensional space and obtain another data matrix as follows:

$$\hat{\mathbf{X}} = \mathbf{T}\mathbf{P}^\mathrm{T} = \mathbf{X}\left(\mathbf{P}\mathbf{P}^\mathrm{T}\right) \quad (20)$$

By simple manipulations (adding and subtracting) in expression (20), the following decomposition of the original data matrix $\mathbf{X}$ can be written:

$$\begin{aligned} \mathbf{X} &= \hat{\mathbf{X}} + \tilde{\mathbf{X}} \\ \hat{\mathbf{X}} &= \mathbf{X}\left(\mathbf{P}\mathbf{P}^\mathbf{T}\right) \\ \tilde{\mathbf{X}} &= \mathbf{X}\left(\mathbf{I} - \mathbf{P}\mathbf{P}^\mathbf{T}\right) \end{aligned} \quad (21)$$

where $\hat{\mathbf{X}}$ is the projection of the data matrix $\mathbf{X}$ onto the selected $r$ principal components and $\tilde{\mathbf{X}}$ is the projection onto the residual left components.

## Applying PCA in practice

To perform PCA is simple in practice through the basic steps:

1. Organize the data set as an $n \times m$ matrix, where $m$ is the number of measured variables and $n$ is the number of trials.
2. Normalize the data to have zero mean and unity variance.
3. Calculate the eigenvectors–eigenvalues of the covariance matrix.
4. Select the first eigenvectors as the principal components.
5. Transform the original data by means of the principal components (projection).

The transformed matrix $\mathbf{T}$ is usually called *score matrix*. Its columns are called *score vectors* $\boldsymbol{t}_i$, each of them associated with the corresponding principal component $\boldsymbol{PC}_i$.

## Damage detection indices

PCA analysis can be used to detect abnormal behavior in a process or system. Two well-known statistics are commonly used to this aim: the $Q$-statistic (or $SPE$-statistic) and the Hotelling's $T^2$-statistic ($D$-statistic). The first one is based on analyzing the residual data matrix $\tilde{\mathbf{X}}$ to represent the variability of the data projection in the residual subspace. The second method is based in analyzing the score matrix $\mathbf{T}$ to check the variability of the projected data in the new space of the principal components. These methods are based on the assumption (generally stemming from the central limit theorem) that the underlying process follows approximately a multivariate normal distribution where the first moment vector is zero (Figure 1).

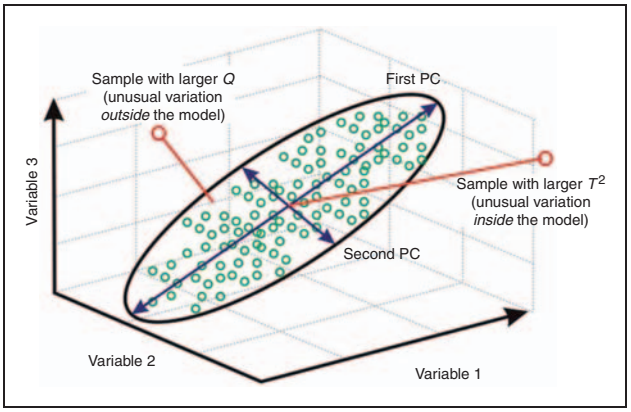


**Figure 1.** PCA model of a three-dimensional data set showing $Q$ and $T^2$ outliers.[27]

### $T^2$-statistic

The Hotelling's $T^2$-statistic is a generalization of Student's $t$-statistic that is used in multivariate hypothesis testing. Consider $\boldsymbol{x}_i$ as the $m$-row vector that represents the measurements from all sensors in the $i$th experiment. Call $\boldsymbol{t}_{si}$ the $r$-row vector (row $i$ within matrix **T)**, which is the projection of the experiment $\boldsymbol{x}_i$ into the new space. Both are related as $\boldsymbol{t}_{si} = \boldsymbol{x}_i\mathbf{P}$.

The $T^2$-statistic of the $i$th sample (or experiment) is defined in the form

$$T_i^2 = \sum_{j=1}^{r} \frac{t_{sij}^2}{\lambda_j} = \boldsymbol{t}_{\mathrm{si}}\Lambda^{-1}\boldsymbol{t}_{\mathrm{si}}^{\mathrm{T}} = \boldsymbol{x}_i\mathbf{P}\Lambda^{-1}\mathbf{P}^{\mathrm{T}}\boldsymbol{x}_i^{\mathrm{T}} \qquad (22)$$

It only detects variation in the subspace of the first $r$ principal components, which are greater than what can be explained by the common-cause variations. In other words, $T^2$-statistic is a measure of the variation of each sample within the PCA model.

Figure 1 gives a conceptual illustration of this index for a case with $m = 3$ variables and $r = 2$ principal components. In this case, $T^2$ is a measure of the variation of each sample within the plane defined by the two principal components.

### $Q$-statistic

$Q$-statistic denotes the change of the events that are not explained by the model of principal components. It is a measure of the difference, or residual between a sample and its projection into the model. The $Q$-statistic of the $i$th sample (or experiment) vector $\boldsymbol{x}_i$ is defined as follows:

$$Q_i = \tilde{\boldsymbol{x}}_i\tilde{\boldsymbol{x}}_i^{\mathrm{T}} = \boldsymbol{x}_i\left(\mathbf{I} - \mathbf{P}\mathbf{P}^{\mathbf{T}}\right)x_i^{\mathrm{T}} \qquad (23)$$

where $\tilde{\boldsymbol{x}}_i$ is its projection into the residual subspace. A conceptual illustration may be seen in Figure 1.

Normally, $Q$-statistic is much more sensitive than $T^2$-statistic. This is because $Q$ is very small and therefore any minor change in the system characteristics will be observable. $T^2$ has great variance and therefore requires a great change in the system characteristic to be detectable.

Information about the events can also be obtained directly from plotting the scores for the relevant principal components. When there is a change in the system, the scores of the new events will be different from the previous scores, and the change will be detected. However, this information is also included in the Hotelling's $T^2$-statistic since it is calculated using the scores. Moreover, the $Q$-statistic supplies additional information that is not included in the scores plot, because it is related to variations that are not considered by the model. In this way, the plots of $Q$ and $T^2$ are hypothesis tests that clearly distinguish experiments with abnormal behavior, whereas the inspection of the scores plot is a qualitative tool.[28]

## Methodology for structural health monitoring

### Data organization and preprocessing

In sections 'Principal component analysis' and 'Damage detection indices', the basis of PCA has been presented considering a matrix $\mathbf{X}$ that contains measurements of several variables for different experiment trials. It has been assumed that each measurement is an individual sample in the data set (just one value). In SHM applications, and specifically in systems based on vibrations, each sensor collects dynamic responses over a whole time period. Then, the result of an

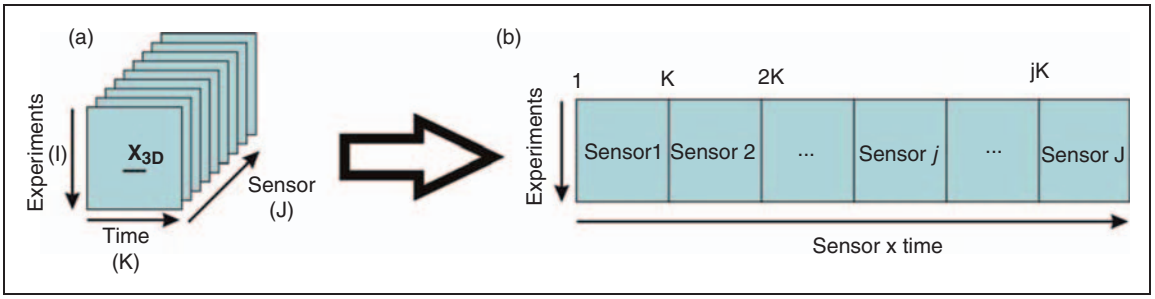


**Figure 2.** Collected data: (a) initial 3D-matrix and (b) unfolded matrix for PCA analysis.

experiment is not a single value, but a set of values obtained by the discretization of the time history measurement.

In this study, the multivariate data set is organized in a three-dimensional matrix $\mathbf{X_{3D}}$ ($I$ experiments $\times$ $K$ samples per experiment $\times$ $J$ sensors). In this way, each frontal slice is a two-dimensional matrix $\mathbf{X}$ that represents all measurements in one sensor as can be seen in Figure 2(a). In order to consider correlations in time for each signal and the correlations between sensors, the matrix $\mathbf{X_{3D}}$ is unfolded as shown in Figure 2(b).[15] This unfolded matrix is the matrix $\mathbf{X}$ to perform PCA analysis.

As explained in section 'Scaling', the first step before applying PCA is to standardize the data matrix $\mathbf{X}$ since PCA is scale variant. For this kind of data sets (unfolded matrices), several studies of scaling have been presented in the literature: continuous scaling (CS), group scaling (GS) and autoscaling (AS).[29] According to these studies, GS is selected for this work because it considers changes between sensors and does not process them independently. Each data-point is scaled using the mean of all measurements of the sensor at the same time (Equation (24)) and the standard deviation of all measurements of the sensor (Equation (25)):

$$\mu_{jk} = \frac{1}{I}\sum_{i=1}^{I} x_{ijk}; \quad \mu_j = \frac{1}{IK}\sum_{i=1}^{I}\sum_{k=1}^{K} x_{ijk} \tag{24}$$

$$\sigma_j^2 = \frac{1}{IK}\sum_{i=1}^{I}\sum_{k=1}^{K}\left(x_{ijk} - \mu_j\right)^2 \tag{25}$$

$$\bar{x}_{ij} = \frac{x_{ij} - \mu_{jk}}{\sigma_j} \tag{26}$$

where:

$x_{ijk}$ is the $k$th sample of the of the $j$th sensor in the $i$th experiment, $\mu_{jk}$ is the mean of the all $k$th samples of the $j$th sensor, $\mu_j$ is the mean of all measurements of the $j$th sensor, $\sigma_j$ is the standard deviation of all measurements of the $j$th sensor, and $\bar{x}_{ij}$ is the scaled sample.

In this way, the mean trajectories (by sensor) are removed and all sensors are made to have equal variance. As a consequence, the experiment trajectories of the sensors and their standard deviations, often nonlinear in nature, are removed from the data.

## General scheme

***Baseline phase.*** *model building*. In systems where diagnosis by pattern recognition is performed, a baseline must be built from data with the system working in the desired normal conditions. In this work, the baseline is created from experiments performed over the healthy structure. PCA is applied to the matrix that contains dynamical responses to a known excitation at different locations. In this setting, all the signals collected from different experiments using the base specimen (undamaged structure) are organized as explained in previous section 'Data organization and preprocessing' (Figure 2). This $\mathbf{X}$ matrix has $I \times KJ$ dimension, where $I$ is the number of experiments, $K$ is the number of samples per experiment and $J$ is the number of sensors. Further, a GS standardization is applied according to Equations (24)–(26). Finally, PCA is applied to the scaled matrix $\mathbf{X}$.

Applying PCA to build a baseline means to calculate the projection matrix $\mathbf{P}$, which offers a better and dimensionally reduced representation of the original data $\mathbf{X}$. This matrix will be the *model* of the undamaged structure to be used in the health diagnosis as illustrated in Figure 3.

***Testing phase.*** *diagnosis*. In this phase, the current structure to diagnose is subjected to a number of experiments and a new matrix $\mathbf{X}$ is arranged with the measured data. The quantity of experiments can be as much as we want, but the numbers of sensors and collected samples (data-points) must be the same that were used in the modeling phase. This matrix is projected into the PCA model with Equation (19). Projections onto some of the first components are obtained and the damage indices ($T^2$-statistic and $Q$-statistic) are calculated and compared with the baseline values. The general

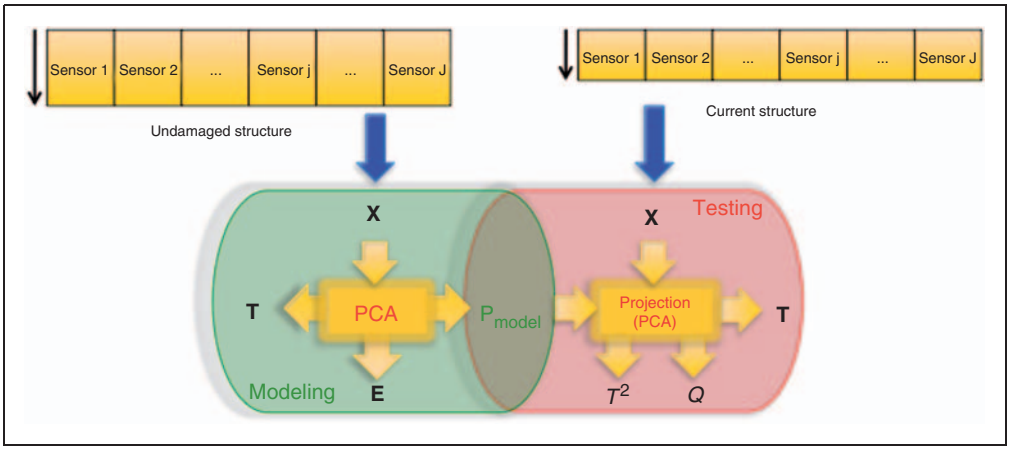


**Figure 3.** General scheme based on PCA for detecting and distinguishing damages in structures.

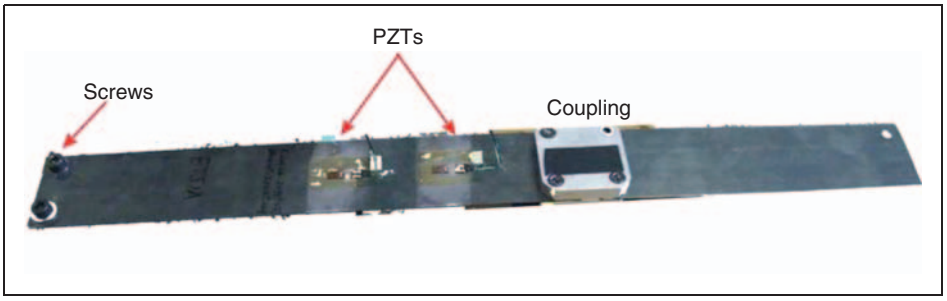


**Figure 4.** Specimen 1: steel sheet.

procedure for detecting and distinguishing damages on structures based on PCA measures can be summarized in Figure 3.

## Experimental set-up

In this study, two structures have been used: (i) a steel sheet, and (ii) a turbine blade of an aircraft. The analysis has been performed in two ways: (i) by exciting at low-frequency vibrations using a shaker in one side of the specimen and measuring data with several PZT sensors attached on the surface, and (ii) by exciting at high-frequency vibrations using one PZT as actuator and the other PZTs as sensors.

### *Steel sheet*

The first specimen is a rectangular steel sheet with nominal dimensions of $510 \times 50\,\text{mm}^2$, it has 1 mm of thickness and it weights 67.3g. Two different screws are attached near the corner in order to break symmetries. The sheet is fixed to a shaker by mean of a coupling. Two PZTs are attached on the surface to collect vibration responses as seen in Figure 4.

**Figure 5.** Steel sheet fixed to the shaker.

The specimen is excited by means of an electromagnetic shaker that converts electrical signals (inputs) to mechanical displacements (Figure 5). The electrical excitation signal is provided by an arbitrary waveform generator and amplified.

A progressive damage was performed on the sheet by mean of a drill: a crack of 2, 4 and 6.8 mm

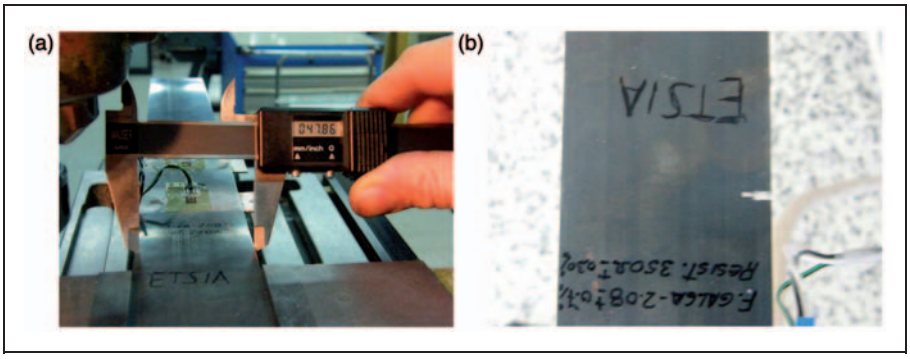


**Figure 6.** (a) Measurement of one of the cracks, and (b) Final specimen damaged.

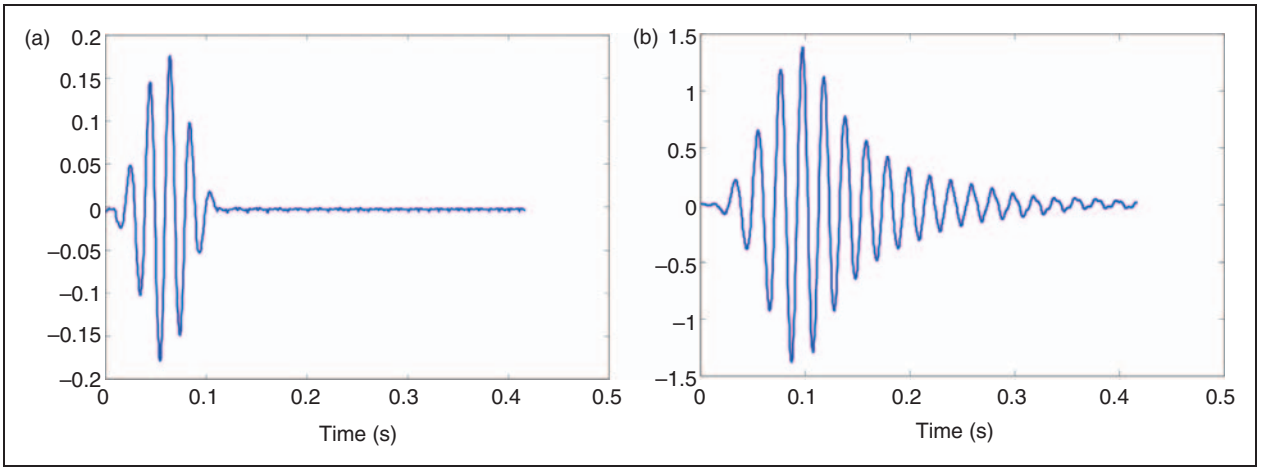


**Figure 7.** (a) Signal excitation, and (b) Measured response.

(Figure 6). The specimen was excited with a sinusoidal signal of low frequency (50 Hz) modulated by a hamming window of five cycles. Figure 7 shows the excitation signal and the response measured by one of the PZTs. A number of 75 experiments were performed using the healthy specimen and 25 of them were used to define the baseline PCA model of the undamaged structure. A number of 50 experiments were performed per each level of the damage in the diagnosis study.

## Blade

This specimen is a turbine blade of a commercial aircraft. Unfortunately, due to the origin of the blade, little is known about the specific material and design parameters constituting the structure. However, it could be determined that the blade is manufactured by a homogenous material with a similar density than titanium (3.57 g/mL). The blade has one stringer in each face. Seven PZT sensors are distributed over the surface to detect time varying strain response data. Three of the sensors are on one face and four on the other face as can be seen in Figure 8. Two kinds of experiments were performed in order to study the effectiveness of the approach for damage detection working at low- and high-frequency vibration.

*Low-frequency vibration.* The blade is suspended by two elastic ropes (free–free configuration). A shaker excites the structure with a vibration signal in one of its extreme ends as seen in Figure 9. The specimen was excited with a sinusoidal signal of low frequency (10 Hz) modulated by a hamming window of five cycles. The signal excitation and the dynamic response of the undamaged structure collected by sensor 2 are shown in Figure 10.

Damages have been simulated adding a mass at four different locations as detailed in Figure 11. A number of 300 experiments have been performed and recorded: 100 with the undamaged structure, and 50 for each one of the four damages. The baseline PCA model was created using half of the data set collected using the undamaged structure. Signals from the other half dataset of the undamaged structure and the whole dataset of the damaged structure were used in the diagnosis testing process.

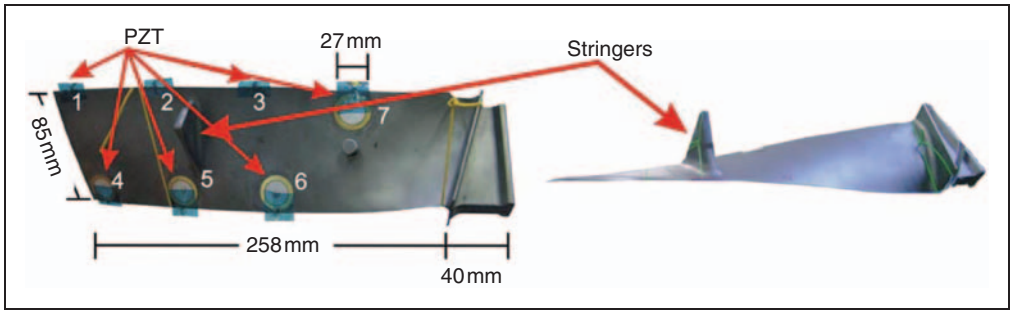


**Figure 8.** Specimen 2: aircraft turbine blade.

**Figure 9.** Blade coupled to the shaker.

*High-frequency vibration.* The blade is also suspended by two elastic ropes (as in the previous configuration). Taking the advantage of the PZTs devices that can be used alternatively as actuators and sensors, PZT 1 was used as actuator and the other PZTs as sensors. The actuator was excited by a burst signal of three peaks and 350 kHz of frequency (Figure 12(a)). A measured signal in one of the PZT is shown in Figure 12(b).

Damages were simulated adding two masses at several locations as shown in Figure 13. 140 experiments were performed and recorded: 50 with the undamaged structure and 10 per each damage. The 80% of the data set collected using the undamaged structure was used for building the baseline. For diagnosis testing, the other 20% of the data set of the undamaged structure and the whole data set of the damaged structure were used.

## Analysis of the results

For each scenario (steel sheet at low frequency, blade at low frequency and blade at high frequency) a PCA model was built with experiments performed using the structure without damage. In this study, the number of principal components to build the model was selected as $r = 20$. In the diagnosis step, the experiments performed using the structure with damages were projected onto the model. Scores 1 against 2 (projections into the first and second principal components, respectively) were plotted. The damage detection indices ($T^2$-statistic and $Q$-statistic) were plotted for each experiment and one versus the other. Shapes and colors represent different conditions of the specimen (healthy, damages 1, 2, ... etc.).

### *Steel sheet: low frequency*

The results for this case are plotted in Figure 14. The first and second scores can be considered as sufficient features to distinguish the different damages. However, some experiments of the damage 1 can not be discerned from some experiments without damage (Figure 14(a)). In this respect, recall that damage 1 is a small crack, just 2 mm. On the other hand, by plotting the damage indices (by experiments or one versus the other), these experiments are clearly separated (Figure 14). From all plots, it is also apparent that experiments with damage 3 are separated in two groups. This has a reasonable explaination: after finishing experiments using the sheet with a 6.8-mm crack (damage 3), we realized that one of the PZTs was broken. Probably after experiment number 26, the PZT broke, and the measurements were corrupted.

### *Blade: low frequency*

The results for this case are plotted in Figure 15. Contrary to the previous case, using the first and second score no trend can be appreciated and it is not possible to classify or cluster the different conditions of the structure (Figure 15(a)). Otherwise, plotting the damage indices some differences can be seen. It can be observed that $Q$-statistic is more sensitive than $T^2$-statistic: undamaged and damages 1 and 4 cases

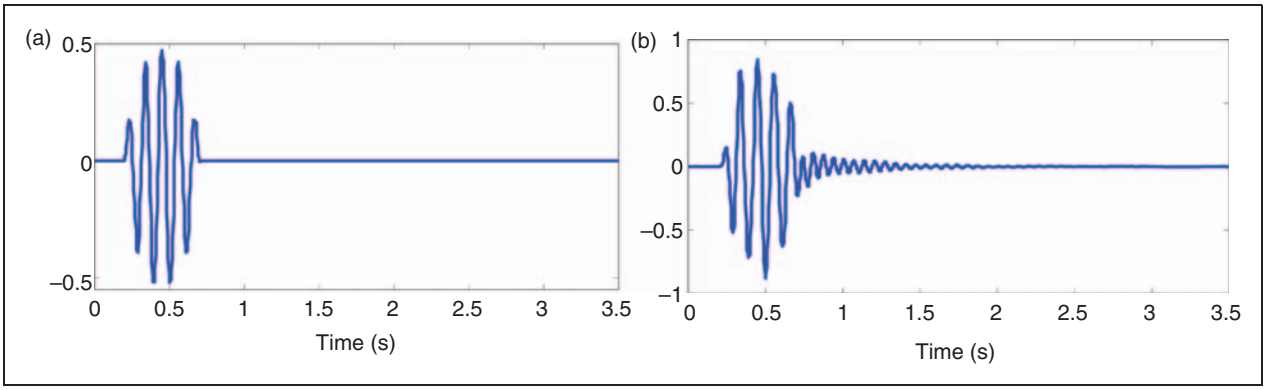


**Figure 10.** (a) Signal excitation, and (b) Dynamical response.

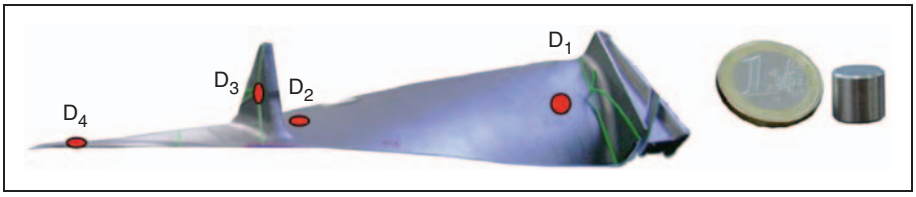


**Figure 11.** Added mass locations

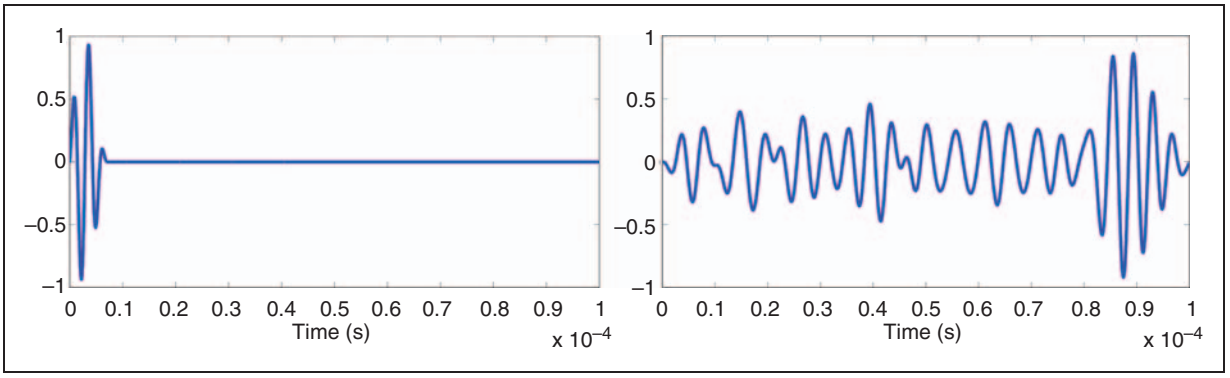


**Figure 12.** (a) Signal excitation, and (b) Dynamical response.

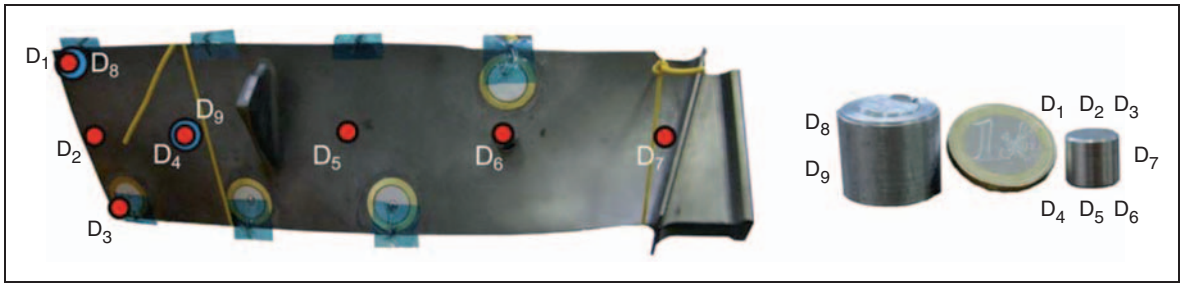


**Figure 13.** Added mass (damage) locations.

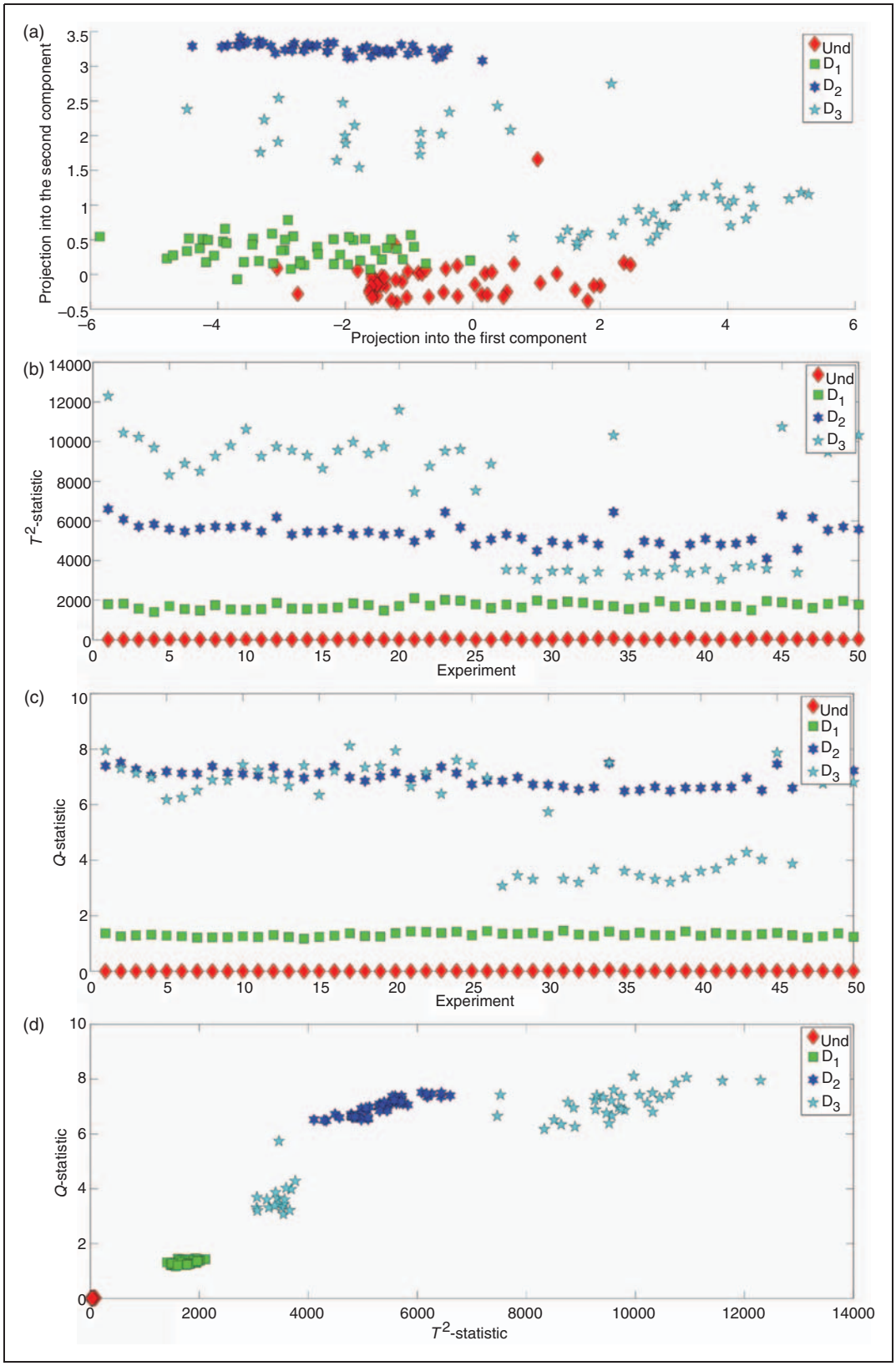


**Figure 14.** Projection of several experiments (undamaged and damaged) into the PCA model: (a) score 1 vs score 2, (b) $T^2$-statistic by experiment, (c) $Q$-statistic by experiment, and (d) $T^2$ vs $Q$.

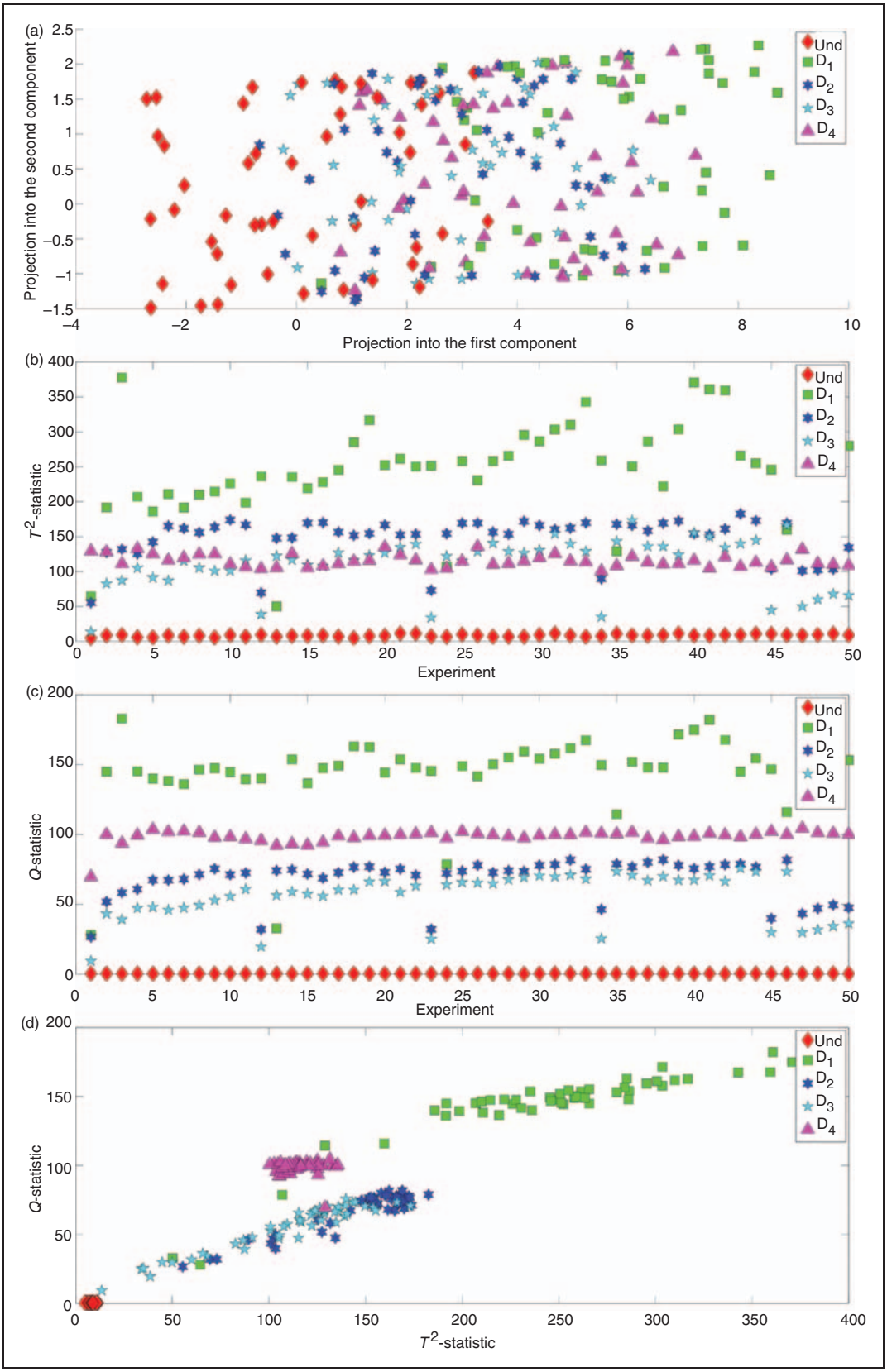


**Figure 15.** Projection of several experiments (undamaged and damaged) into the PCA model: (a) score 1 vs score 2, (b) $T^2$-statistic by experiment, (c) $Q$-statistic by experiment, and (d) $T^2$ vs $Q$.

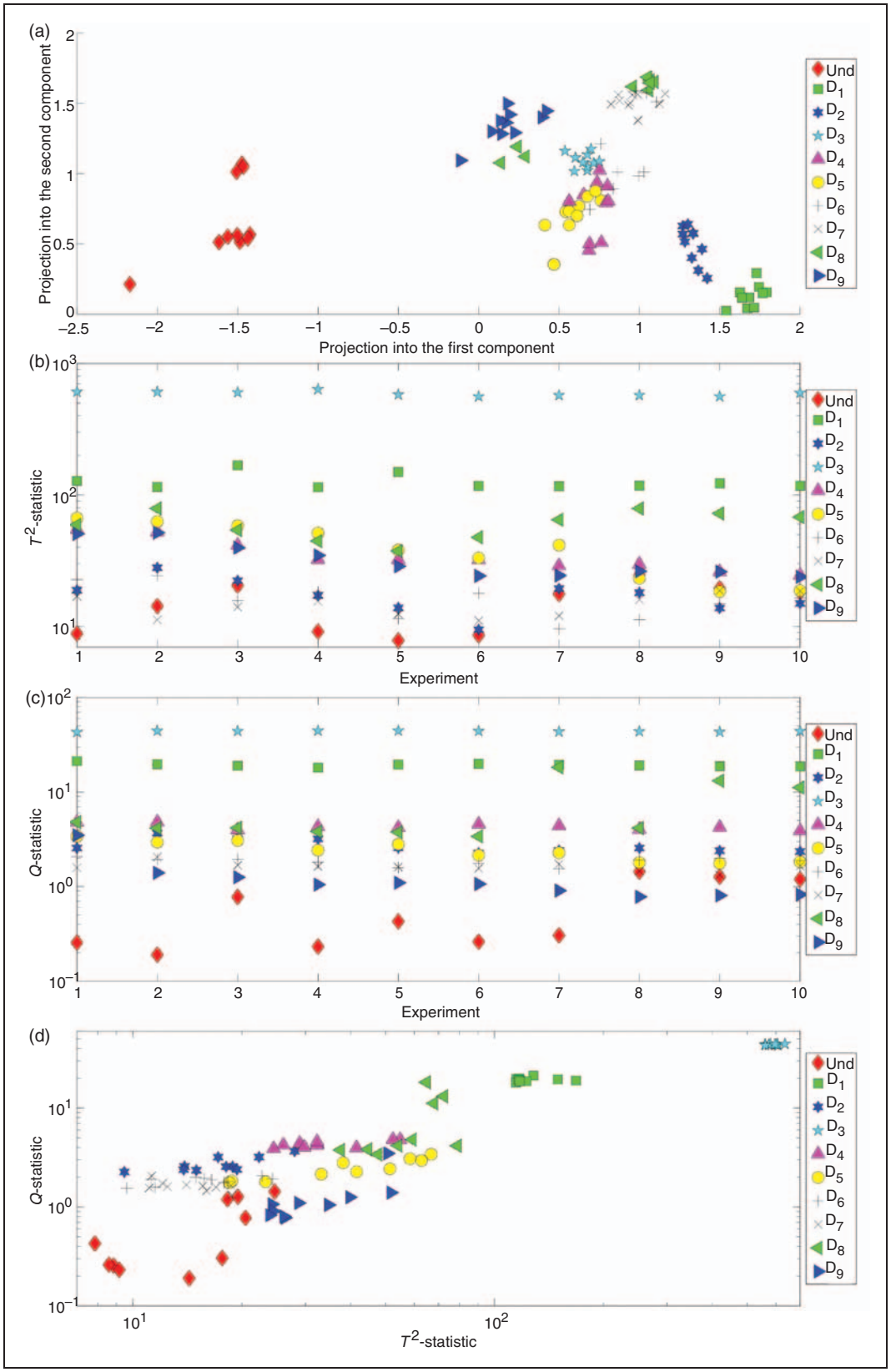


**Figure 16.** Projection of several experiments (undamaged and damaged) into the PCA model: (a) score 1 vs score 2, (b) $T^2$-statistic by experiment, (c) $Q$-statistic by experiment, and (d) $T^2$ vs $Q$.

are clearly distinguished using only $Q$-statistic but damages 2 and 3 appear very close. In this respect, it is worth to note (Figure 11) that damage 3 is located over the stringer and damage 2 is very close, which poses a practical difficulty for the precise detection. Indeed, the added mass (or lost mass) is small comparing with the mass that distorts the propagation of the wave (the stringer).

### *Blade: high frequency*

Figure 16 shows the results for this case. At a first glance, it is observed in Figure 16(a) that the discrimination between the presence and the absence of damage in the blade is clearly achieved in all the cases by using just the first two projections (scores 1 and 2). In a more detailed view of Figure 16, some damages are distinguishable from the others: damages 1, 2, and 9 appear clearly in separate groups in the scores plots, while damages 1, 3, and 9 do it when using the indices plots. Other damages are grouped although not easily separable from the others.

Some interpretations are possible for the above observations. First, notice that only one excitation is applied to the blade by means of the PZT1, which is located at a blade corner (Figure 8). As seen in Figure 13, damages 5, 6, and 7 are located behind the stringer. This stringer is a large quantity of mass that may significantly distort the wave propagation. Therefore, these damages are detectable but hardly distinguishable. Notice also that damages 4 and 5 are symmetrically located with respect to the stringer. This may explain that, as seen in Figure 16(a), damages 4 and 5 appear quite overlapped. If experiments with damages 5, 6, and 7 were removed from the data set, Figure 16 would be much clearer than the present one, and damages would appear easily separated from the others. But it may be interesting to highlight the difficulty and challenge of distinguishing damages by means of a signal processing based approach (without a physical analysis of the wave propagation process) when the shape of the structure has portions that may significantly affect the wave propagation.

In the context of this discussion, it may be interesting to revisit the low-frequency experiments of section ''Blade: low frequency'' and to consider the case where damage is present near the base of the blade, which is the most distant location with respect to the actuating excitation location. This damage is number 1 in the low-frequency case (Figure 11) and number 7 in the high-frequency experiments (Figure 13). It is noticed in Figure 15 that this damage is distinguishable at low frequency, while it is overlapped with other damages under high frequency wave excitation (Figure 16). Trying to explain this fact, notice that, at low frequency, the vibration produced by the shaker is larger (in amplitude) than the produced by the PZT at high frequency. In the first case the stringer does not significantly distort the propagation of the vibration, so the damage 1 (even being far from the excitation) is easily detected and distinguished from the undamaged structure and the other damages.

## Concluding remarks

In order to detect and discern damages in structures using vibrations by mean of the application of PCA and $T^2$ and $Q$-statistic indices, several scenarios were experimentally analyzed. The difficulty level was increasing with the scenarios; the first specimen studied was a simple structure (steel sheet) with small, but clear defects (real cracks). Further, the effectiveness of the approach was tested using a more complex structure in both low and high frequency. At low frequency, few defects were simulated and it was concluded that damages very near to the stringer are detectable but not easily distinguishable. This can be explained because the added mass is small comparing with the mass of the stringer. For experiments at high frequency, those defects were eliminated and others were added (seven different positions and two different masses).

In some cases, scores are sufficient features to discern damages. In other cases, $T^2$-statistic is more sensible to changes in the structure while in other cases $Q$-statistic is better. In cases where neither $T^2$-statistic nor $Q$-statistic is efficiently enough separately, it may be convenient to represent one versus the other in the same plot (Figures 14(d), 15(d), and 16(d)). In general, it is advisable to analyze all indices and scores as a whole set to obtain more accuracy in the diagnosis (or classification) of damages. The authors are developing strategies that allow to reach a consensus from all these features.

Independently of the used structure and the kind of excitation, experiments have demonstrated that the first level for SHM is accomplished: all cases with damage have been detected. Its projections are clearly discerned from the experiments with the healthy structure. Separation among different damages has been reasonably achieved in locations where the dynamic response is not significantly affected by the stringer. At high frequency, the stringer acts a barrier (or obstacle) for the wave propagation. To avoid this problem, work is in progress by the authors with the aim of extending the present approach using more PZTs as actuators, taking advantage of their reversibility, and developing strategies to handle the whole set of information for an enhanced diagnosis.

## Acknowledgments

This work has been supported by the 'Ministerio de Ciencia e Innovación' in Spain through the coordinated research project DPI2008-06564-C02-01/02, and the post-doctoral programme 'Juan de la Cierva'. The authors thank the support from the 'Agència de Gestió d'Ajuts Universitaris i de Recerca' of the 'Generalitat de Catalunya', 'Universitat Politécnica de Catalunya' and 'Universidad Politécnica de Madrid'. We are also grateful to Professor Jesús López-Diez for his valuable suggestions and ideas during the experimental phase.

## References

1. Worden K and Farrar CR. Structural Health Monitoring. Theme issue of. *Philos Trans R Soc: Ser A* 2007; 365: 539–560.
2. Doebling W, Farrar CR, Prime MB and Shevitz DW. Damage identification and health monitoring of structural and mechanical systems from changes in their vibration characteristics: a literature review. Los Alamos National Laboratory Report LA-13070-MS, Los Alamos, NM. 1996.
3. International Workshop on Structural Health Monitoring. Since 1997.
4. European Workshop on Structural Health Monitoring. Since 2002.
5. World Conference on Structural Control and Monitoring. Since 2000.
6. Structural Control and Health Monitoring. http://www3.interscience.wiley.com/journal/117861846/group-home/home.html.
7. *Structural Health Monitoring. An International Journal*. Available at: http://shm.sagepub.com/
8. Staszewski WJ, Boller C and Tomlinson GR. *Health monitoring of aerospace structures: smart sensor technologies and signal processing*. Chichester, England: John Wiley & Sons, Ltd, 2004.
9. Adams D. *Health monitoring of structural materials and components*. New York, NY: John Wiley & Sons, 2007.
10. Farrar CR, Doebling SW and Nix DA. Vibration-based structural damage identification. *Philos Trans R Soc Ser A* 2001; 359: 131–149.
11. McCullagh P. What is a statistical Model? *Ann Stat* 2002; 30(5): 1225–1310.
12. Jolliffe IT. *Principal component analysis*. Springer series in statistics, 2nd ed. New York: Springer, 2002.
13. Worden K and Manson G. Visualization and dimension reduction of high-dimensional data for damage detection. *IMAC* 1999; 17: 1576–1585.
14. Zang C and Imregun M. Structural damage detection using artificial neural networks and measured FRF data reduced via principal component projection. *J Sound Vib* 2001; 242(5): 813–827.
15. Mujica LE, Vehí J, Ruiz M, Verleysen M, Staszewski W and Worden K. Multivariate statistics process control for dimensionality reduction in structural assessment. *Mech Syst Signal Process* 2008; 22: 155–171.
16. Yan AM, Kerschen G, De Boe P and Golinval JC. Structural damage diagnosis under varying environmental conditions—part II: local PCA for non-linear cases. *Mech Syst Signal Process* 2005; 9: 865–880.
17. Park S, Lee JJ, Yun CB and Inman DJ. Electro-mechanical impedance-based wireless structural health monitoring using PCA-data compression and k-means clustering algorithms. *J Intell Mater Syst Struct* 2007; 19(4): 509–520.
18. Sophian A, Tian GY, Taylor D and Rudlin J. A feature extraction technique based on principal component analysis for pulsed Eddy current NDT. *NDTE Int* 2003; 36: 37–41.
19. Tang J. Frequency response based damage detection using principal component analysis. In: *IEEE International Conference on Information Acquisition*, Hong Kong, China, June 27 to July 3, 2005, pp.407–412.
20. Zhong A, Song H and Han B. Extracting structural damage features: comparison between PCA and ICA. In: Huang DS, Li K and Irwin G eds. *Intelligent computing in signal processing and pattern recognition*, Lectures notes in control and informatic, Vol. 345. Berlin/Heidelberg: Springer, 2006, pp.840–845.
21. Sohn H, Czarnecki JA and Farrar CR. Structural health monitoring using statistical process control. *J Struct Eng* 2000; 126(1): 1356–1363.
22. De Boe P and Golinval JC. Principal component analysis of a piezosensor array for damage localization. *Struct Health Monitor J* 2003; 2(2): 137–144.
23. Golinval JC, De Boe P, Yan AM and Kerschen G. Structural damage detection based on PCA of vibration measurements. In: *Proceedings of the 58th Meeting of the Society for Machinary Failure Prevention Technology On CD*, Virginia, 2004.
24. Mustapha F, Worden K, Pierce SG and Manson G. Damage detection using stress waves and multivariate statistics: an experimental case study of an aircraft component. *Strain* 2007; 43(1): 47–53.
25. Trendafilova I, Cartmell MP and Ostachowicz W. Vibration-based damage detection in an aircraft wing scaled model using principal component analysis and pattern recognition. *J Sound Vib* 2008; 313(3): 560–566.
26. Johnson M. Waveform based clustering and classification of AE transients in composite laminates using principal components analysis. *NDTE Int* 2002; 35: 367–376.
27. Wise BM, Gallagher NB, Butler SW, White D and Barna GG. Development and benchmarking of multivariate statistical process control tools for a semiconductor etch process: impact of measurement selection and data treatment on sensitivity. In: *IFAC SAFEPROCESS '97*, Kingston Upon Hull, UK, 1997, pp.35–42.
28. Qin SJ. Statistical process monitoring: basics and beyond. *J Chemometrics* 2003; 17: 480–502.
29. Westerhuis J, Kourti T and MacGregor J. Comparing alternative approaches for multivariate statistical analysis of batch process data. *J Chemometrics* 1999; 13: 397–413.